

Polymer Electrolyte Membrane Fuel Cell Characterisation Based on Current Distribution Measurements

S. Chevalier^a, J.-C. Olivier^b, C. Josset^a, and B. Auvity^a

^a Laboratoire de Thermique et Énergie de Nantes (CNRS UMR 6607), Polytech Nantes, Université de Nantes, La Chantrerie, rue Christian Pauc, Nantes, France.

^b IREENA Laboratory, Université de Nantes, Saint-Nazaire, France

In this work, a methodology to characterize polymer electrolyte membrane (PEM) fuel cell mass transport phenomena is described. A segmented fuel cell with two straight channels is used to measure the current density distribution along the channel. A one-dimensional current density distribution model is also developed to analyze the measurement. This model is first validated at low current density where the current density distribution is function of the oxygen stoichiometry only, and then used at high current density (around 0.1 V) to measure the mass transport resistance. Good agreement between our measurements based on current density distribution and the literature is reported. The measured mass transport resistances are found to be constant regardless the inlet air mass flow rate, concluding to the robustness of our methodology.

Introduction

Alternative engines to convert and store energy which do not produce any greenhouse gas are a must need. Among the large variety of processes such as wind turbine or solar panel, Polymer Electrolyte Membrane (PEM) fuel cells are one of the most promising candidate. They convert hydrogen and air into electricity and heat with water as the only bi-product. The efficiency of the direct conversion of the chemical energy into electrical energy is also an important asset of this technology. Today, PEM fuel cells are close to the commercialization, but their cost still needs to be decrease to reach the full market deployment. To decrease the fuel cell cost, the electrical power density has to be increased. This can be achieved by both improving the electrochemistry (1) and the mass transport in all the fuel cell materials (2).

The improvement of the mass transport in fuel cell relies on several aspects: (i) improved understanding of the physics governing the transport of air, water and hydrogen in each fuel cell component, (ii) improved experimental methods to characterize the mass transport phenomena, and (iii) identification of specific fuel cell operating regimes where fuel cell performances are governed by the mass transport. The identification of specific operating regime is of great importance to enable the characterization of the dominating physical phenomena and to build simplified fuel cell models. For instance, Kulikovskiy (3) reported catalyst layers (CL) regimes where the current density distribution models within the CL thickness are derived. Following this path, specific fuel cell operating regimes were described in authors' previous works (4) where it was shown that fuel cell current density distribution is governed by the oxygen stoichiometry at low/moderate current density and mass transport resistance (Peclet number) at high/limiting current. A

direct application of these findings is to make available relatively simple models of current density distribution, and to use them to both design or characterize PEM fuel cell.

In this paper, we report the use of current density measurements to characterize fuel cell mass transport phenomena. A segmented fuel cell is specifically designed and built to measure current density distributions as well as to allow optical access to anode and cathode channels in order to visualize liquid water if any. The current density measurements are performed at low and high current density, and are compared to the corresponding model. At high current density, we show how the diffusive resistance of oxygen in fuel cell porous materials can be measured under relatively low oxygen stoichiometry.

Methods

Current density distribution model

The development of the model is fully detailed in author's previous work (4), but the main assumptions are summarized here. It is based on four fundamental processes that governed the electrochemical conversion of hydrogen into electricity: the oxygen transport in the channel and in the GDL, the charge transport in the PEM, and the electrochemical reaction in the catalyst layer (CL). The anode is neglected here since it is assumed that it does not limit the fuel cell performance. In these conditions, the fuel cell geometry is reduced to a half-cell as depicted in Figure 1. The particular aspect ratio of fuel cells lets us consider that the oxygen transport is purely 1D in the y -direction in the channel and in the x -direction in the GDL. Similar assumptions have been drawn in pseudo 2D fuel cell models (5) or 1D+1D fuel cell models (6).

The other main assumptions of the model concern the transport of liquid water and the value of the fuel cell parameters. In the present model, the liquid water is not explicitly modelled. It is considered that its impact can be seen through the value of the fuel cell parameters, such as the PEM ohmic resistance or the GDL effective diffusivity among others. In addition, fuel cell parameters are considered to be effective values which are constant along the channel (y -direction).

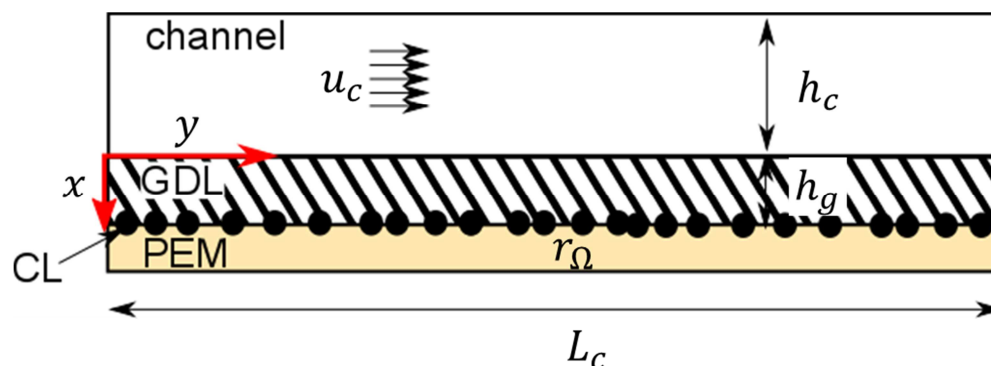


Figure 1. Schematic of the half-cell used for the model.

To simplify the calculations and the model, we also consider that the fuel cell is isothermal with ideal current collectors (no ohmic losses in them). The oxygen transport in the channel is assumed to be a plug-flow with an averaged air velocity, u_c . In addition,

a plane CL is considered at the cathode meaning that the electrochemical reaction takes place homogeneously throughout the CL thickness. This last assumption is valid in case of rapid oxygen and charge transport in the CL (3). Thus, under all these assumptions, one can depict a PEM fuel cell as in Figure 1 where the main transport phenomena are reported at the cathode.

The dimensionless distribution of the current density along the channel associated with the simplified PEM fuel cell depicted in Figure 1 can be written as (4):

$$-\text{Pe} \frac{d\tilde{j}(\tilde{y})}{d\tilde{y}} = \frac{\tilde{j}(\tilde{y})}{1 + \frac{1}{\text{Da}} \left(1 + \frac{\tilde{j}(\tilde{y})}{\text{Wa}}\right) e^{\frac{\tilde{j}(\tilde{y})}{\text{Wa}}}} \quad [1]$$

where $\tilde{j} = j/j_0$ is the dimensionless current density distribution, $j_0 = j(0)$ is the inlet current density. Equation (1) is governed by three dimensionless numbers defined as:

- The Peclet number $\text{Pe} = u_c h_c h_g / (D^{eff} L_c)$ which compares the ratio of oxygen transported in the channel to the mass transport in fuel cell porous media;
- The Damköhler number $\text{Da} = i_c e^{(E^0 - E)/b} / (4F c^{ref} D^{eff} / h_g)$ which compares the kinetics of the reaction to diffusive flux of oxygen in the GDL;
- The Wagner number $\text{Wa} = b / (r_\Omega j_0)$ which compares the voltage losses in the CL to the voltage losses in the membrane.

The stoichiometric regime. Equation (1) has no analytical solution in the present general form, but it was shown that analytical solutions exist in specific regimes defined according to the dimensionless number values (4). In particular, at low current density and fast oxygen transport in the GDL the Wagner number is large ($\text{Wa} \gg 1$) when the Damköhler number is small ($\text{Da} \ll 1$). In these conditions,

$$\tilde{j}(\tilde{y}) = e^{-\lambda^* \tilde{y}}, \quad [2]$$

where λ^* is the ratio of Da to Pe which writes:

$$\frac{\text{Da}}{\text{Pe}} = \frac{i_c e^{(E^0 - E)/b} L_c}{4F c^{ref} u_c h_c} \approx \frac{j_0 L_c}{4F c^{ref} u_c h_c}. \quad [3]$$

The expression $i_c e^{(E^0 - E)/b}$ is found to be equal to j_0 in this regime since the concentration gradient in the GDL is very small as well as the membrane resistance (4). Then, to find the expression of λ^* , we first compute the mean current density produced by the cell as

$$I_{cell} = j_0 \int_0^1 \tilde{j}(\tilde{y}) d\tilde{y} = j_0 / \lambda^* (1 - e^{-\lambda^*}). \quad [4]$$

Rearranging Equation (4) leads to

$$\frac{I_{cell} \lambda^*}{j_0} = \frac{I_{cell} L_c}{4F c^{ref} u_c h_c} = \lambda^{-1}. \quad [5]$$

where λ is the oxygen stoichiometry. Finally, the parameter λ^* can be linked to λ as

$$\lambda^* = -\ln(1 - \lambda^{-1}). \quad [6]$$

By combining Equations (2), (4) and (6), an expression of the current density distribution which depends only on the oxygen stoichiometry can be found as

$$j(\tilde{y})/I_{cell} = \lambda^* \lambda e^{-\lambda^* \tilde{y}}. \quad [7]$$

A similar expression for the current density distribution was reported by Kulikovsky (7).

The oxygen diffusion limiting regime. Following the same methodology, an analytical solution of the current density distribution in the oxygen diffusion limiting regime is derived. In this regime, the Damköhler number can be considered large (i.e. $Da > 20$) and Equation (1) has the following analytical solution:

$$\tilde{j}(\tilde{y}) = j(y)/j_0 = e^{-\tilde{y}/Pe}. \quad [8]$$

Then the mean current density is computed as:

$$I_{cell} = j_0 \int_0^1 \tilde{j}(\tilde{y}) d\tilde{y} = j_0 Pe (1 - e^{-1/Pe}). \quad [9]$$

Combining Equation (8) and (9) leads to

$$\frac{j}{I_{cell}} = \frac{e^{-\tilde{y}/Pe}}{Pe(1 - e^{-1/Pe})}. \quad [10]$$

Equation (10) shows that the distribution j/I_{cell} is a function of the Peclet number only. Thus current density distribution measurements can be used to identify the Peclet number and then the effective GDL diffusivity. A nonlinear inverse method must be used to fit Pe onto the experimental data. The Matlab[®] subroutine *fminsearch* was used. Once the value of the Peclet number is identified, the mass transport resistance in the fuel cell is computed as:

$$R_d = \frac{h_g}{D^{eff}} = \frac{L_c}{u_c h_c} Pe. \quad [11]$$

It has to be noted that R_d represents the total mass transport resistance in the fuel cell including the diffusive phenomena in all the porous media (GDL, MPL and CL). The standard deviation associated to the identified value of R_d , σ_{R_d} , is computed as:

$$\sigma_{R_d} = R_d \frac{\sigma_{Pe}}{Pe}, \quad [12]$$

where σ_{Pe} is the standard deviation of Pe obtained from the residue of the inverse method, χ , and the sensitivity vector, S , as

$$\sigma_{Pe} = \sqrt{\chi/9[S^T S]^{-1}}, \quad [13]$$

where χ is the Euclidian norm between the model and the experimental data, the subscript T indicates the transposed vector, and 9 arises from the difference between the number of data (11 points) minus the number of parameters (1 parameter, Pe) minus 1 (see ref.(4)). The sensitivity vector, S , related to the Peclet number is computed as:

$$S = \frac{\partial}{\partial Pe} \left(\frac{j}{I_{cell}} \right) = \frac{e^{-\tilde{y}/Pe}}{Pe^3(1 - e^{-1/Pe})} \left(\tilde{y} + \frac{e^{-1/Pe}}{1 - e^{-1/Pe}} - Pe \right), \quad [14]$$

Segmented single cell

A 12 cm² (200 mm by 6 mm) single cell was specially designed to measure the current density distribution and the mass transport resistance. It comprises two parallel channels of 200 mm length. At the cathode side, the flow field was machined directly in the copper current collector to enable an optical access inside the channels via a transparent plexiglass plate inserted on the top of the channels. The channels dimensions are 1.5 mm width by 0.5 mm height. At the anode side a segmented current collector was used to measure the current density distribution (see Figure 2). This current collector was built directly onto a printed circuit board (PCB). Between the current collectors, a membrane electrode assembly (MEA) was inserted; it is made of a 15 μm-thick Gore PEM with 0.5 mg/cm² platinum loading in both anode and cathode CL. The thin membrane and high platinum loading were specially chosen to ensure low membrane resistance and efficient electrochemical reaction. The MEA was sandwiched between two 10BC GDLs from SGL[®] compressed at 250 μm using two rigid spacers (40% of compressed ratio). Finally, two aluminum end-plates were used to assemble all the fuel cell components. A water cooling circuit connected to a temperature control system was drilled inside the end plates to keep the fuel cell temperature constant. More details about our experimental setup can be found in authors' previous work (8).

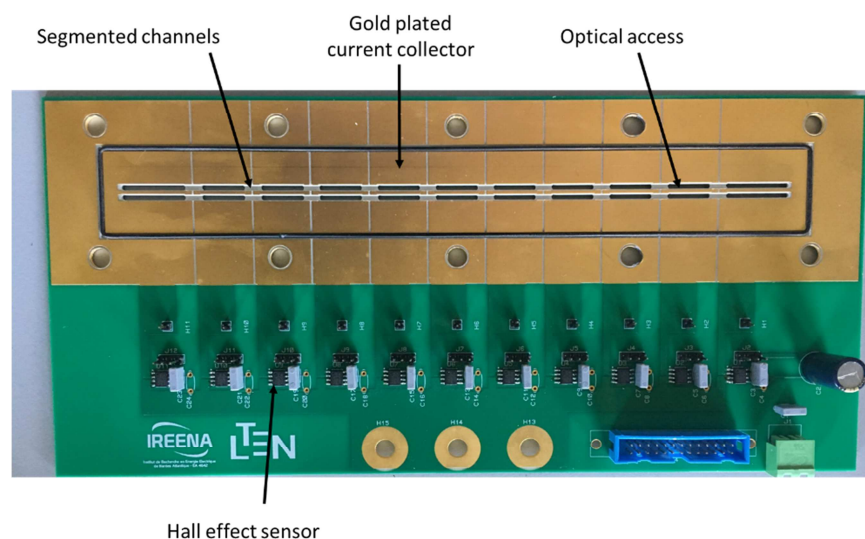


Figure 2. Photography of the segmented current collector used to measure the current density distribution along the channels.

The segmented current collector comprises 11 segments of 18 mm which corresponds to a surface of 1.08 cm² each (see Table 1). Each segment is linked connected in series to a Hall effect sensor (Allegro Microsystem, ACS723LLCTR-05AB-T) which converts the current that flows through the segment into voltage. All the 11 voltages are then read by a data acquisition system every second. According to the data sheet of the sensor and all the experimental uncertainty, it is assumed that the current densities are measured with an accuracy of ±10%. Thus, the uncertainty associated to the ratio j/I_{cell} based on uncertainty propagation rule writes:

$$\sigma_{j/I_{cell}} = \sqrt{2/100} j/I_{cell} , \quad [15]$$

The experimental oxygen stoichiometry and air velocity in the channel are computed from the operating conditions. The model derived in the previous section is based on a

two dimensional (2D) geometry which does not take in to account the effect of the rib. Therefore, the velocity defined in the Peclet number is a 2D velocity that would flow in the cell in absence of rib. Experimentally, the 2D velocity is given by

$$u_c^{2D} = \frac{\dot{Q}(T, p)}{l_c h_c}, \quad [16]$$

where l_c is the cell width, e.g. 6 mm. Then, the oxygen stoichiometry is obtained experimentally as:

$$\lambda = \frac{\dot{Q}(T, p)c^{ref}}{I_{cell}/(4F)}. \quad [17]$$

TABLE I. Characteristics of segments in the segmented collector. The air inlet is located at the segment 11 and the outlet at the segment 1. The fuel cell is fed in counter flow conditions.

Segment #	1	2	3	4	5	6	7	8	9	10	11
Length (mm)	19	18	18	18	18	18	18	18	18	18	19
Area (cm ²)	1.14	1.08	1.08	1.08	1.08	1.08	1.08	1.08	1.08	1.08	1.14
Dimensionless position	0.9525	0.86	0.77	0.68	0.59	0.5	0.41	0.32	0.23	0.14	0.0475

Results & Discussion

Validation of the methodology

A first set of experiments was performed to validate our methodology: i.e. both the measurements of the current density distribution and the associated model. It was shown that at low current density, the current density distribution obeys to a simple law which depends on the oxygen stoichiometry only (see Equation (7)). Thus, current density distributions are measured between 3 and 6 A (0.25 and 0.5 A/cm², respectively) for a range of oxygen stoichiometry. Table II summaries the operating conditions used. It has to be noticed that only the oxygen stoichiometry and current density were varied, all the other operating parameters were kept constant.

TABLE II. Operating conditions of the measurements at low current density. The temperature was kept constant at 70 °C. Air is dry, and hydrogen was humidified at 30% at 70°C. Hydrogen flow rate was set to 300 ml/min.

Current (A)	Flow rate (ml/min)	Pressure (bar)	Stoichiometry
6	54	1.90	1.25
6	65	2.00	1.54
6	89	1.94	2.05
6	131	2.01	3.05
4.5	40	1.98	1.25
4.5	49	1.97	1.54
3	27	1.98	1.25
3	33	2.02	1.54
3	43	2.01	2.05

The results are presented in Figure 3 where the measurements are compared to the model for the same oxygen stoichiometry. In Figure 3(a), it is shown that regardless the

mean current used to perform the measurements, the same j/I_{cell} distributions are observed. This result validates that the distributions of current density obey only to the stoichiometry. Moreover, the comparison with the analytical model shows that the correct current density distribution trend is predicted by the model. Similar results are observed in Figure 3(b) to (d) validating our model.

A small discrepancy can be seen between the model and the experimental data in the first segments ($\tilde{y} < 0.2$). Several assumptions can explain such results, i.e. during the fuel cell assembly process the GDL can be slightly misplaced at the inlet leading to a wrong estimate of the current density in these segments. The change in PEM water content in the first segments can also impact the current density distribution (6,9) which would also explain this small discrepancy. However, the assumption of constant membrane resistance along the channel seems to be acceptable since our model is able to well predict the current density distribution.

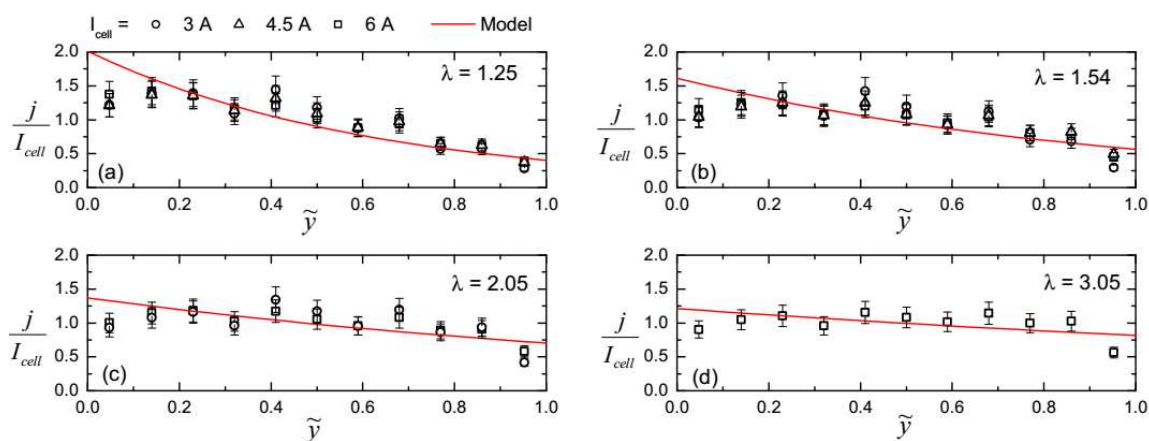


Figure 3. Comparison of the current density distributions measured for a range of current density and oxygen stoichiometry and the model (equation 7). The Figure (a) to (d) depict the current density distribution for a range of oxygen stoichiometry of 1.25, 1.54, 2.05 and 3.05, respectively.

Mass transport resistance measurements

The second set of experiments was performed at high current density. The cell voltage was kept constant at 0.1 V while the current density distribution was measured for a range of air flow rates (see Table III). The air flow rates correspond roughly to oxygen stoichiometries between 2 and 1.2. During the experiments it was checked that no liquid water was present in the channel. This was done through the optical access machined in the current collectors.

The results of the non-linear fit of the Peclet number are presented in Figure 4 for three channel velocities. It is observed that the current density distributions are well fitted using Equation (10) regardless the channel velocity. There are still small discrepancies in the first segments, but in general the exponential decrease of current density distribution is well captured by our model.

The mass transport resistance and their associated standard deviation are then computed from the fitted values of Pe . These results are presented in Table III. It is

observed that the more accurate value of R_d is obtained when the channel velocity is the slowest. In this condition, the exponential decrease of the current density is more pronounced increasing the sensitivity of Pe and therefore enhancing its identification. Concerning the value of R_d , even though a small decrease of resistance is obtained when the channel velocity decreases, this is not significant regarding their associated standard deviation. It is more reasonable to conclude that the mass transport resistance is almost constant around 8 s/cm. This value is in the range of literature, i.e. Muirhead et al. (10) reported mass transport resistance values around 2 s/cm for a fuel cell with SGL 25BC GDL compressed at 25%. Taking into account that our GDL is slightly thicker and more compressed ($\sim 40\%$), the measured R_d are typically in the expected range of values. Moreover, the 1D mass transport resistance can be estimated to be $4Fc^{ref}/I_{cell} \approx 6.5$ s/cm which is in close agreement to the measured R_d validating our methodology.

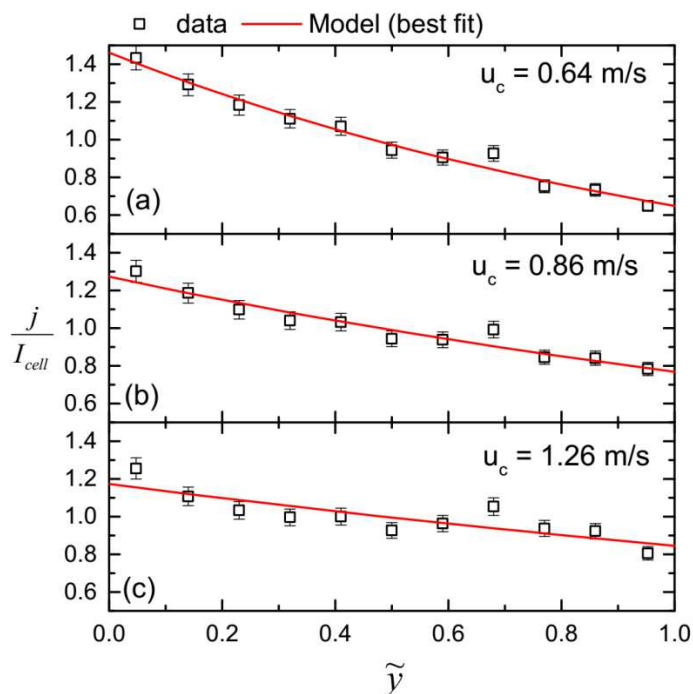


Figure 4. Results of the fit of the Peclet number for three air channel velocity: 0.64 m/s (a), 0.86 m/s (b), and 1.26 m/s (c). All the other operating conditions were kept constant during the measurements.

TABLE III. Operating conditions of the measurements at high current density. The temperature was kept constant at 70 °C. Air is dry, and hydrogen was humidified at 30% at 70°C. The cell voltage was kept at 0.1 V

Current (A)	Flow rate (ml/min)	Pressure (bar)	2D velocity (m/s)	Pe	R_d (s/cm)
15.5	227	1.96	1.26	3.05±1.47	9.67±4.66
14.1	155	1.96	0.86	1.98±0.50	9.26±2.33
13.2	116	1.95	0.64	1.23±0.18	7.63±1.12

Conclusions

A new methodology to characterize fuel cell mass transport phenomena based on the current density measurement is reported in this work. A segmented current collector was built for a fuel cell with two straight channels. The optical access enables to verify the absence of liquid water in the channel and therefore to derive a simple current density distribution model. This model was validated at low current density where fuel cell physics is mainly governed by the oxygen stoichiometry. A good agreement between the 1D current density model and the experimental data for a range of cell current is reported.

The fuel cell mass transport resistance is then measured at high current under 0.1 V fuel cell voltage. This resistance includes all the diffusive resistance in the fuel cell porous media (GDL, MPL, and CL in particular). In these conditions, the current density distribution depends on the Peclet number from which R_d is directly obtained. As predicted by our model, the current density distribution presents an exponential decrease along the channel in this operating regime. The value of R_d obtained using our method is in agreement with the data reported in the literature and with the classical method used to measure the 1D mass transport resistance. Nonetheless, our methodology enables mass transport resistance measurements under low oxygen stoichiometry which is more representative of the real application. Moreover, the measurements performed in 2D with our methodology are more accurate than using the 1D mass transport resistance measurements since the complete distribution of current is used, not a single value of current.

More investigations will follow this work using other sets of GDLs, and for a range of fuel cell voltage between 0.4 and 0.1 V to specify the limits of our methodology.

Acknowledgments

The research leading to these results received funding from the People Programme (Marie Curie Actions) of the European Union's Seventh Framework Programme (FP7/2007-2013) under REA grant agreement n° PCOFUND-GA-2013-609102, through the PRESTIGE programme coordinated by Campus France. The authors would like to gratefully acknowledge Mr Christophe Le Bozec for his help in designing and building the experimental setup.

References

1. M.J. Eslamibidgoli, J. Huang, T. Kadyk, A. Malek, M. Eikerling, *Nano Energy*. **29** (2016) p. 334.
2. A.Z. Weber, R.L. Borup, R.M. Darling, P.K. Das, T.J. Dursch, W. Gu, et al., *J. Electrochem. Soc.* **161** (2014) p. F1254.
3. A.A. Kulikovskiy, *Electrochim. Acta*. **55** (2010) p. 6391.
4. S. Chevalier, C. Josset, B. Auvity, *Renew. Energy*. **125** (2018) p. 738.
5. G. Maranzana, J. Mainka, O. Lottin, J. Dillet, A. Lamibrac, A. Thomas, S. Didierjean, *Electrochim. Acta*. **83** (2012) p. 13.
6. A.A. Kulikovskiy, *Electrochem. Commun.* **6** (2004) p. 969.
7. A.A. Kulikovskiy, *Electrochim. Acta*. **49** (2004) p. 617.
8. S. Chevalier, C. Josset, B. Auvity, *J. Power Sources*. (2018), (submitted).

9. I.A. Schneider, S.A. Freunberger, D. Kramer, A. Wokaun, G.G. Scherer, *J. Electrochem. Soc.* **154** (2007) p. B383.
10. D. Muirhead, R. Banerjee, J. Lee, M.G.M.G. George, N. Ge, H. Liu, S. Chevalier, J. Hinebaugh, K. Han, A. Bazylak, *Int. J. Hydrogen Energy.* **42** (2017) p. 29472.